Available online at www.sciencedirect.com
SCIENCE DIRECT®
Journal of Organometallic Chemistry 690 (2005) 3765–3773
Journal of Organometallic Chemistry
www.elsevier.com/locate/jorganchem

Rhenium carbonyl complexes with monodentate-coordinated diphosphines: activation of terminal phosphino groups towards amine-oxide oxidation

Wei Fan [a], Rui Zhang [a], Weng Kee Leong [b], Chit Kay Chu [a], Yaw Kai Yan [a,*]

[a] *Natural Sciences & Science Education, National Institute of Education, Nanyang Technological University, 1 Nanyang Walk, Singapore 637616, Republic of Singapore*

[b] *Department of Chemistry, National University of Singapore, 3 Science Drive 3, Singapore 117543, Republic of Singapore*

Received 18 April 2005; received in revised form 9 May 2005; accepted 9 May 2005
Available online 21 June 2005

Abstract

Terminal phosphino groups of $[Re_2(CO)_9(\eta^1\text{-P-P})]$ (P-P = diphosphines) are activated towards oxidation by Me_3NO. The respective reactions of Me_3NO with $[Re_2(CO)_9\{\eta^1\text{-P}(o\text{-anisyl})_2(CH_2)_3PPh_2\}]$, $[Re_2(CO)_9\{\eta^1\text{-}PPh_2(CH_2)_3P(o\text{-anisyl})_2\}]$ and $[Re_2(CO)_9(\eta^1\text{-}trans\text{-}PPh_2CH{=}CHPPh_2)]$ were studied to investigate the mechanism of this oxidation. The results are consistent with an intramolecular pathway involving a cyclic intermediate, without exchange of the coordinated and terminal phosphino groups. A mechanism which involves an interaction of the terminal phosphino group with a carbonyl ligand is proposed. In sharp contrast to *eq*-$[Re_2(CO)_9(\eta^1\text{-P-P})]$ (P-P = $Ph_2P(CH_2)_nPPh_2$, n = 1–6), *eq*-$[Re_2(CO)_9(\eta^1\text{-}trans\text{-}PPh_2CH{=}CHPPh_2)]$ appears to be indefinitely stable towards equatorial → axial isomerization at room temperature, thus, allowing its crystal structure to be determined.

Keywords: Rhenium; Carbonyl; Monodentate diphosphines; Amine-oxide; Phosphine-oxide complexes; Equatorial isomer

1. Introduction

Reactions of the complexes $[Re_2(CO)_9(\eta^1\text{-P-P})]$ (P-P = $Ph_2P(CH_2)_nPPh_2$, n = 1–6) with Me_3NO yield the close-bridged complexes $[Re_2(CO)_8(\mu\text{-P-P})]$ and phosphine-oxide complexes $[Re_2(CO)_9\{\text{P-P(O)}\}]$ (Fig. 1) as major products [1]. Whilst the formation of close-bridged products can be easily explained by Me_3NO-assisted decarbonylation followed by phosphine coordination, it is not clear how the phosphine-oxide complexes are formed. This oxidation reaction has been observed in the reaction of $[Re_2(CO)_9(\eta^1\text{-dppf})]$ [dppf = 1,1′-bis(diphenylphosphino)ferrocene] with Me_3NO, but no mechanism was proposed [2]. Since free diphosphines do not react with Me_3NO under similar conditions, the phosphine-oxide complexes could not have been formed by a straightforward oxygen-transfer from the amine-oxide to the uncoordinated phosphino group.

A plausible mechanism for the formation of the phosphine-oxide complexes (Mechanism 1, Scheme 1) involves the interaction of the uncoordinated phosphorus atom with the electron-deficient carbon atom of a CO ligand. This reduces the electron density on phosphorus, facilitating nucleophilic attack by Me_3NO. A net electron flow from the electron-rich carbonyl oxygen to the electron-deficient nitrogen then follows, resulting in the formation of the phosphine-oxide complex and trimethylamine. It is noteworthy that an intramolecular P–CO interaction has been observed in the complex $[W(CO)_5(\eta^1\text{-dppm})]$ (dppm = $Ph_2PCH_2PPh_2$), in which

* Corresponding author. Tel.: +65 6 790 3821; fax: +65 6 896 9414.
E-mail address: ykyan@nie.edu.sg (Y.K. Yan).

0022-328X/$ - see front matter © 2005 Elsevier B.V. All rights reserved.
doi:10.1016/j.jorganchem.2005.05.010

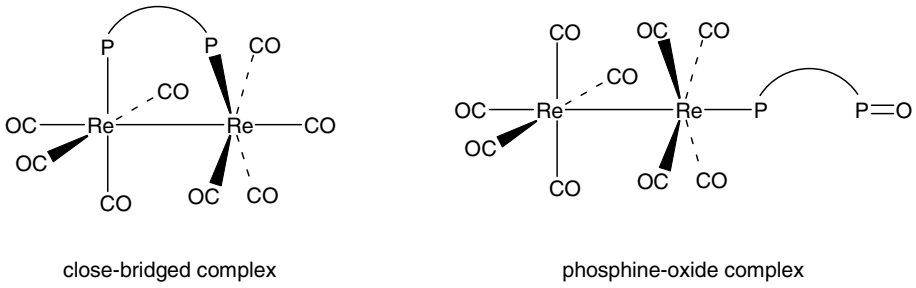

Fig. 1. General structures of the close-bridged and phosphine-oxide complexes.

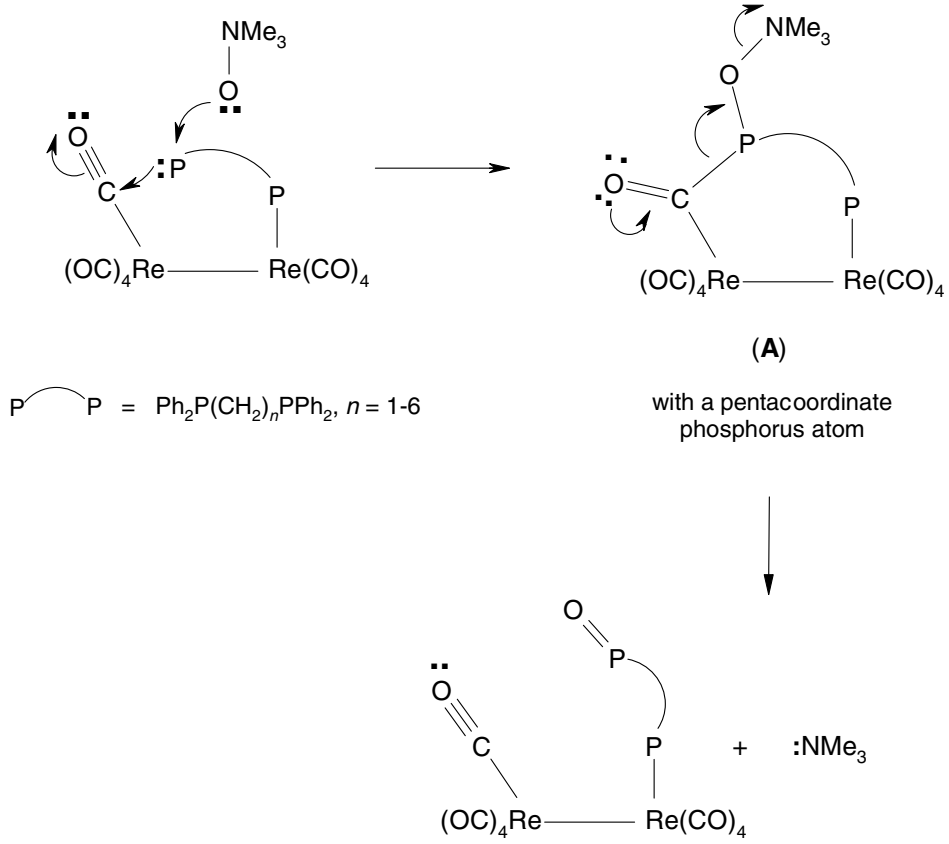

Scheme 1.

the lone pair of the terminal phosphino group is oriented towards one of the *cis*-CO groups (P···C distance = 3.5 Å), and there is ^{13}C (*cis*-CO)–^{31}P (terminal) coupling [3]. Another possible mechanism (Mechanism 2, Scheme 2) involves nucleophilic attack of Me_3NO on the coordinated phosphorus atom, which is then displaced by the terminal phosphino group. The coordinated phosphorus is activated towards attack by the amine-oxide since it is less electron-rich compared to the uncoordinated phosphorus atom. Intramolecular exchange of coordinated and terminal phosphino groups has been observed in $[(OC)_5WPPh_2CH_2CH(PPh_2)_2]$, $[(OC)_5MPPh_2CH_2CH_2\{P(p\text{-tolyl})_2\}]$ and $[(OC)_5M\{P(p\text{-tolyl})_2CH_2CH_2PPh_2\}]$ (M = Cr, Mo, W) [4,5].

The above mechanisms were tested by studying the reactions of Me_3NO with the dirhenium nonacarbonyl complexes of monodentate-coordinated *trans*-1,2-bis-(diphenylphosphino)ethene (dppene) and 1-(di-*o*-anisylphosphino)-3-(diphenylphosphino)propane (dadpp), $Ph_2P(CH_2)_3P(o\text{-anisyl})_2$. Mechanism 2 requires the diphosphine to adopt a chelating conformation in transition-state **B**, which would not be possible for dppene.

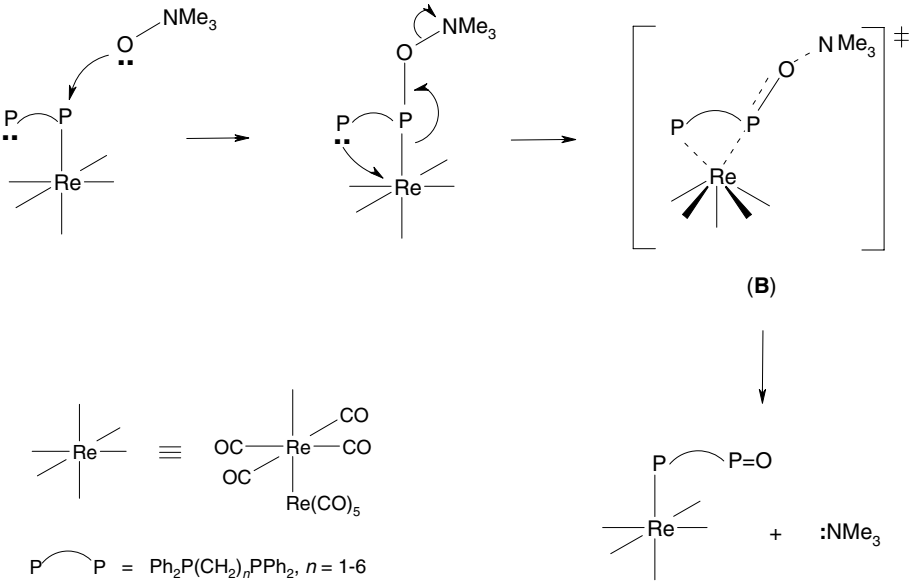

Scheme 2.

Mechanism 1, on the other hand, requires the diphosphine to adopt an A-frame-like conformation, which is possible for dppene [6]. Hence, if Mechanism 2 is correct, no phosphine-oxide complex would be observed for dppene. In addition, Mechanism 2 would result in the originally coordinated phosphino group being oxidized, and the originally terminal phosphino group coordinating to the metal, which would be observable for the dadpp complexes $[Re_2(CO)_9\{\eta^1\text{-}P(o\text{-anisyl})_2\text{-}(CH_2)_3PPh_2\}]$ (**1**) and $[Re_2(CO)_9\{\eta^1\text{-}PPh_2(CH_2)_3P\text{-}(o\text{-anisyl})_2\}]$ (**2**). If Mechanism 1 is correct, however, the originally terminal phosphino group would be the one oxidized.

The reaction of $[Re_2(CO)_9(\eta^1\text{-dppm})]$ with $[ReO_4]^-$ was also carried out to investigate the possible involvement of $[ReO_4]^-$ in the formation of the phosphine-oxide complex. It has been reported that the reaction of $[Re_2(CO)_{10}]$ with a large excess of Me_3NO (8.4×) in THF for 24 h gives the perrhenate salt $[Re(CO)_3(ONMe_3)_3][ReO_4]$ in 9% yield [7]. It is therefore possible that the reaction of $[Re_2(CO)_9(\eta^1\text{-P-P})]$ with Me_3NO may generate some $[ReO_4]^-$, which in turn oxidizes the terminal phosphino group.

2. Results and discussion

2.1. Synthesis and characterization of $[Re_2(CO)_9(\eta^1\text{-P-P})]$ (P-P = dadpp, dppene)

The complexes $[Re_2(CO)_9(\eta^1\text{-P-P})]$ (P-P = dadpp, dppene) were synthesized by reactions of the diphosphines with $[Re_2(CO)_{10}]$ and Me_3NO. As in the analogous reactions of $Ph_2P(CH_2)_nPPh_2$ ($n = 1$–6) [1], mixtures of $[Re_2(CO)_9(\eta^1\text{-P-P})]$ (monodentate complexes) and $[\{Re_2(CO)_9\}_2(\mu\text{-P-P})]$ (dimer complexes) were formed.

For dadpp, two monodentate complexes, $[Re_2(CO)_9\{P(o\text{-anisyl})_2(CH_2)_3PPh_2\}]$ (**1**) and $[Re_2(CO)_9\{PPh_2\text{-}(CH_2)_3P(o\text{-anisyl})_2\}]$ (**2**) were obtained. The ^{31}P NMR spectrum of **1** shows two equally intense singlets at −8.3 and −17.5 ppm, respectively. The lower-field signal could be assigned to the anisyl-bonded phosphorus atom coordinated to the $[Re_2(CO)_9]$ moiety, and the higher-field signal can be assigned to the uncoordinated, phenyl-bonded phosphorus atom [cf. δ_p ($CDCl_3$, ppm) for $Ph_2P(CH_2)_3PPh_2 = -17.5$; for $P_aPh_2(CH_2)_3P_b(o\text{-anisyl})_2$, $P_a = -16.7$, $P_b = -37.1$]. Complex **2** exhibits two singlets (−11.7 and −35.8 ppm), corresponding to the coordinated phenyl-bonded phosphorus and the uncoordinated anisyl-bonded phosphorus atoms, respectively. The dimer complex $[Re_2(CO)_9\{P(o\text{-anisyl})_2\text{-}(CH_2)_3PPh_2\}Re_2(CO)_9]$ (**3**) gives two signals [4.3 (PPh_2) and −5.2 {$P(anisyl)_2$} ppm] in its ^{31}P NMR spectrum. It is evident that the ^{31}P shift of the coordinated Ph_2P group in **2** is very different from that of the Ph_2P group in **3**. This difference can be explained by the fact that the Ph_2P group is coordinated equatorially in **2**, but axially in **3** (the Re–Re bond being the molecular axis). In general, the ^{31}P resonance for the axial isomer always occurs 10–20 ppm downfield of the equatorial isomer for $[Re_2(CO)_9(PR_3)]$ complexes [8]. The anisyl-bonded phosphorus atoms in **1** and **3** are both in the axial position, as indicated by their large coordination shifts ($\delta_{coord} - \delta_{free} = \Delta\delta$) of +28.8 (for **1**) and

+31.9 ppm (for **3**), cf. $\Delta\delta$ = +22.9 ppm for *ax*-[$Re_2(CO)_9(\eta^1$-dppf)] [2].

Conversion of *eq*-**2** to its axial isomer occurs readily in solution at room temperature. For example, after incubating a CH_2Cl_2 solution of *eq*-**2** at room temperature under nitrogen for a week, only *ax*-**2** was detected [δ_P = 4.5 and −35.8 ppm]. This isomerization could also be accomplished in refluxing toluene within 10 min. The fast equatorial–axial isomerization of **2**, and the isolation of the axial isomers of **1** and **3** are consistent with the observation by others that monosubstitution of [$Re_2(CO)_{10}$] with phosphines usually results in axially substituted products [9].

Reaction of dppene with [$Re_2(CO)_{10}$] and Me_3NO gives the monodentate complex *eq*-[$Re_2(CO)_9(\eta^1$-dppene)] (**4**) and the dimer complex *diax*-[{$Re_2(CO)_9$}$_2$(μ-dppene)]. Interestingly, despite the bulkiness of dppene, complex **4** appears to be indefinitely stable as the equatorial isomer in solution at room temperature, and can only be converted into the axial isomer by heating in toluene. This provided a unique opportunity to grow single crystals of an equatorial [$Re_2(CO)_9(\eta^1$-P-P)] complex for X-ray crystallography (see below).

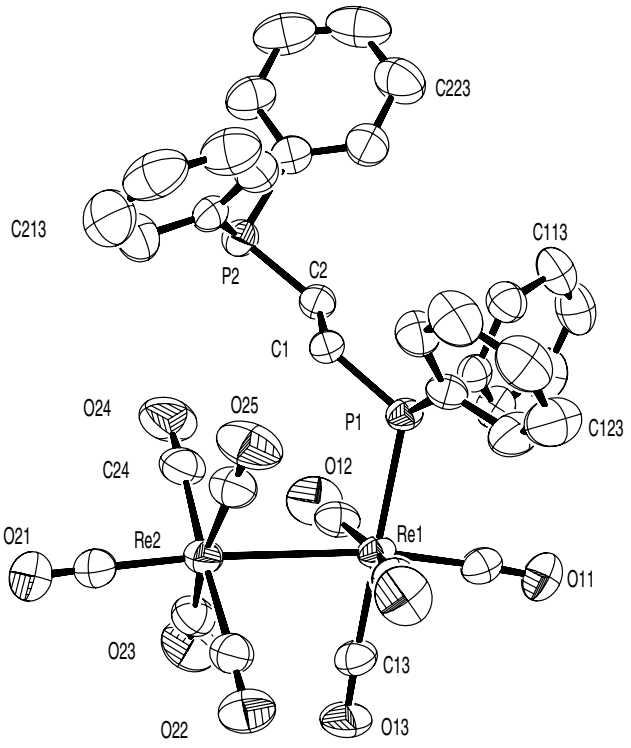

Fig. 2. Crystal structure of *eq*-[$Re_2(CO)_9(\eta^1$-dppene)] (**4**)

2.2. Crystal structure of [$Re_2(CO)_9(\eta^1$-dppene)] (**4**)

The two Re octahedra in the molecule of **4** (Fig. 2) are approximately staggered, being rotated from the C(13)–C(22) eclipsed position by 49.2°. The presence of the phosphine on the equatorial position probably precludes an ideal staggered form.

Viewed down the P(1)–Re(1) direction, the backbone of the dppene ligand is rotated clockwise from the eclipsed position with the Re–Re bond, giving a C(1)–P(1)–Re(1)–Re(2) torsional angle of 26.2°. This rotation directs C(1) close to the equatorial carbonyl group [C(24)–O(24)] and causes this CO group to bend away from the Re–Re bond. The C(1)···C(24) distance is 3.389 Å, slightly less than twice the van der Waals radius of carbon, and the Re(1)–Re(2)–C(24) angle [93.0(2)°] is much larger than the Re–Re–C angles of the other equatorial carbonyl groups [average 83.6(2)°]. Despite the short C(1)···C(24) distance, there is no evidence for electronic interaction between the C=C bond of the diphosphine with the carbonyl group, the C(1)–C(2) bond length [1.334(5) Å] being normal for a C–C double bond. There is also a very short contact of 3.291 Å between C(121) and C(14), the phenyl ring [C(121)–C(126)] and the carbonyl group [C(14)–O(14)] being almost eclipsed. The C(121)–P(1)–Re(1)–C(14) torsional angle is only 10.7°, compared with the C(111)–P(1)–Re(1)–C(11) torsional angle of 34.1°.

There are no short contacts between P(2) and any of the carbonyl groups, the shortest P···O distance being 3.516 Å [P(2)···O(24)] and the shortest P···C distance being 4.262 Å [P(2)···C(24)]. These distances are larger than the sum of van der Waals radii of the relevant elements. The lack of short P···C contacts in the crystal of **4** does not, however, preclude P···C interaction in short-lived intermediates (e.g., intermediate **A** in Scheme 1) in solution.

The only reported structurally characterized equatorial [$Re_2(CO)_9(PR_3)$] complex is *eq*-[$Re_2(CO)_9(PPh_2H)$] [10]. Compared with this compound, complex **4** is clearly very strained. This is most evident from the Re–Re–P angle [99.79(2)°], which is much larger than the corresponding angle [91.77(8)°] of *eq*-[$Re_2(CO)_9(PPh_2H)$], and the acute Re–Re–C(NR) angles of equatorially coordinated isonitrile complexes [11,12]. The Re–P bond length of **4** [2.4887(9) Å] is also longer than that in *eq*-[$Re_2(CO)_9(PPh_2H)$][2.443(3) Å]. The steric strain in **4** could also be partially responsible for the lengthening of the Re–Re bond [3.1077(2) Å], compared to those in *eq*-[$Re_2(CO)_9(PPh_2H)$] [3.0526(7) Å] and [$Re_2(CO)_{10}$] [3.041(1) Å] [13].

2.3. Reactions of complexes **1** and **2** (axial isomers) with Me_3NO

As expected, a close-bridged complex and a phosphine-oxide complex were obtained from each of the above reactions. The ^{31}P NMR spectra of the two phosphine-oxide complexes, **5** and **6**, each shows two equally intense singlets. Complex **5** (δ_P −7.2 and 32.7 ppm), iso-

lated from the reaction of **1** with Me_3NO, is identified as *ax*-[$Re_2(CO)_9${P(*o*-anisyl)$_2$(CH_2)$_3$P(O)Ph_2}] (30% yield), while complex **6** (δ_P 4.8 and 33.3 ppm), isolated from the reaction of **2** with Me_3NO, is identified as *ax*-[Re_2-$(CO)_9${$PPh_2(CH_2)_3$P(O)(*o*-anisyl)$_2$}] (27%). To confirm these structural assignments, oxidation reactions of **1** and **2** by oxygen were also carried out. Exposure of a CH_2Cl_2 solution of **1** to air for one week at room temperature gave a product whose ^{31}P shifts were identical to those of **5**. Similar treatment of **2** gave **6** as the sole product. These observations clearly show that there is no exchange between the coordinated and free phosphino groups in the reactions of **1** and **2** with Me_3NO.

The close-bridged complexes isolated from the reactions of **1** and **2** with Me_3NO were identical and identified to be *dieq*-[$Re_2(CO)_8$(μ-dadpp)]. The IR spectrum of this complex in the carbonyl stretching region is similar to that of *dieq*-[$Re_2(CO)_8$(μ-dppp)] [1] [dppp = $Ph_2P(CH_2)_3PPh_2$]. Its ^{31}P NMR spectrum shows two equally intense doublets (J_{P-P} = 30 Hz) at −10.4 and −20.2 ppm, respectively, the relatively large negative δ_P values being consistent with the compound being a [$Re_2(CO)_8$(μ-P-P)] complex with a seven-membered metallacycle (cf. δ_P = −17.5 ppm for *dieq*-[$Re_2(CO)_8$(μ-dppp)]) [1]. That the non-coupled phosphorus atoms in free dadpp become coupled to each other in *dieq*-[Re_2-$(CO)_8$(μ-dadpp)] further confirms the close-bridged structure of the latter. The formation of *dieq*-[Re_2-$(CO)_8$(μ-dadpp)] from *ax*-**1** and -**2** shows that axial → equatorial isomerization is possible.

2.4. Reaction of [$Re_2(CO)_9(\eta^1$-dppene)] with Me_3NO

Reaction of *eq*-[$Re_2(CO)_9(\eta^1$-dppene)] with Me_3NO produces the phosphine-oxide complex *eq*-[Re_2-$(CO)_9${η^1-$PPh_2CH{=}CHP(O)Ph_2$}] [δ_P 22.6(d) and −5.9(d) ppm, J_{P-P} = 36 Hz] in 14% yield and an unusual complex, [$Re_2(CO)_8$(μ-$OPPh_2CH{=}CHPPh_2$)] (**7**) in 19% yield. The reaction of *ax*-[$Re_2(CO)_9(\eta^1$-dppene)] with Me_3NO is much slower than that of the equatorial isomer, and gives mainly the axially substituted phosphine-oxide complex (δ_P 23.2 and 8.7 ppm, J_{P-P} = 45 Hz) and an unidentified, unstable complex.

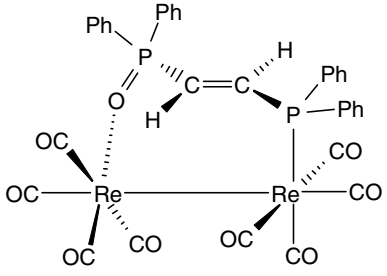

7

The structure of **7** was deduced mainly from its ^{31}P NMR and mass spectra. There are two coupled doublets (J_{P-P} = 4.5 Hz) at 26.3 and −23.6 ppm, respectively, in its ^{31}P NMR spectrum. The signal at 26.3 ppm is most likely the resonance of the phosphoryl group, and the signal at −23.6 ppm can be assigned to the phosphino group. The very negative ^{31}P shift for the latter is also consistent with its being part of a seven-membered metallacycle [1]. The FAB mass spectrum of the complex shows its M^+ ion at *m*/*z* 1008, together with a $[M + H]^+$ peak at *m*/*z* 1009, with overlapping isotope patterns. The IR spectrum of **7** is consistent with its assigned structure, there being five ν_{CO} absorptions, with the highest-energy absorption (2091 cm^{-1}) occurring at a lower frequency than that of *eq*-[$Re_2(CO)_9${$PPh_2CH{=}CHP(O)Ph_2$}] (2104 cm^{-1}). Complex **7** is most likely formed via Me_3NO-assisted decarbonylation of *eq*-[$Re_2(CO)_9${$PPh_2CH{=}CHP(O)$-Ph_2}], followed by coordination of the phosphoryl oxygen to rhenium.

2.5. Mechanistic implications

The lack of exchange between the coordinated and terminal phosphino groups of **1** and **2** and the formation of dppene-oxide complexes from **4** confirm that Mechanism 2 is incorrect. Focusing on Mechanism 1, it would appear from Scheme 1 that, for the axial isomers of **1**, **2** and **4** to react with Me_3NO to form phosphine-oxide complexes, they must either isomerize back to the equatorial isomers, or the terminal phosphino group must interact with a CO ligand on the P-coordinated rhenium (proximal CO) rather than one on the adjacent Re atom. From the foregoing discussion, it may be assumed that back-and-forth axial–equatorial isomerization is much more facile for **1** and **2** than for **4**. Due to its flexible backbone, dadpp is also much better able than dppene to bend to allow its uncoordinated phosphino group to interact with a proximal CO ligand. It is thus not surprising that the yields of phosphine-oxide complexes from *ax*-**1** and -**2** are much higher than that from *ax*-**4**, and that better yields of phosphine-oxide complexes are obtained from *eq*-**4** than *ax*-**4**. Overall, the dependence of the yields on chain flexibility and position of substitution is consistent with an intramolecular pathway involving a cyclic intermediate (Scheme 1).

2.6. Reaction of eq-[$Re_2(CO)_9(\eta^1$-dppm)] with perrhenate

Like the reactions of **1**, **2** and **4** with Me_3NO, the reaction of *eq*-[$Re_2(CO)_9(\eta^1$-dppm)] with [NBu_4][ReO_4] was carried out in THF under N_2 at room temperature for 4 h. Much unreacted *eq*-[$Re_2(CO)_9(\eta^1$-dppm)] was recovered, and a small amount of the equatorial

phosphine-oxide complex, *eq*-[$Re_2(CO)_9$(dppmO)] (15% yield based on the consumed starting material) was formed. Free dppm does not react with [NBu_4][ReO_4] under the same conditions.

The above results show that the perrhenate ion can indeed oxidize (albeit very slowly) *eq*-[$Re_2(CO)_9(\eta^1$-dppm)] to the phosphine-oxide complex. However, since the quantity of $[ReO_4]^-$ formed in the Me_3NO reactions should be very small compared to that reported in [7], given the stoichiometric amount of Me_3NO used and shorter reaction time, its role in the formation of the phosphine-oxide complexes should be negligible. Furthermore, the failure of $[ReO_4]^-$ to oxidize free dppm suggests that, even if $[ReO_4]^-$ plays a significant part in the formation of the phosphine-oxide complex, the mechanism should also involve the rhenium carbonyl units, and is not a direct oxygen-transfer between $[ReO_4]^-$ and the phosphino group.

3. Conclusions

Terminal phosphino groups of [$Re_2(CO)_9(\eta^1$-P-P)] (P-P = diphosphines) are activated towards oxidation by Me_3NO. This oxidation yields [$Re_2(CO)_9${P-P(O)}], which is most likely formed via an intramolecular pathway involving a cyclic intermediate. Exchange of coordinated and terminal phosphino groups does not occur during the reaction. A mechanism which involves an interaction of the terminal phosphino group with a carbonyl ligand is proposed. Perrhenate does not play a significant role in the formation of the phosphine-oxide complexes. In sharp contrast to *eq*-[$Re_2(CO)_9(\eta^1$-P-P)] (P-P = $Ph_2P(CH_2)_nPPh_2$, n = 1–6), *eq*-[$Re_2(CO)_9(\eta^1$-*trans*-$PPh_2CH{=}CHPPh_2$)] appears to be indefinitely stable towards equatorial → axial isomerization at room temperature.

4. Experimental

4.1. General

All reactions were routinely performed under pure dry nitrogen using standard Schlenk techniques. All solvents for the reactions were also vacuum degassed before use. The solvents were of reagent grade and were freshly purified and dried by published procedures [14]. Chemical reagents, unless otherwise stated, were commercial products and were used without further purification. Pre-coated silica TLC plates of layer thickness 0.25 mm were purchased from Merck. The diphosphine $Ph_2P(CH_2)_3P(o$-anisyl$)_2$ (dadpp) was synthesized by the method of Benn et al. [15]. Fourier-transform infrared spectra were recorded with a Perkin–Elmer 1725X FT-IR Spectrometer. Phosphorus-31 NMR spectra were recorded at room temperature on a Bruker DRX400 spectrometer at 162 MHz. The phosphorus chemical shifts are quoted from the proton-decoupled spectra, and are reported in ppm to the higher frequency of external 85% H_3PO_4. Fast atom bombardment mass spectra were recorded on a VG AutoSpecQ mass spectrometer using a 3-nitrobenzyl alcohol matrix. Elemental analyses were performed using a LECO CHNS-932 instrument.

4.2. Synthesis of [$Re_2(CO)_9(\eta^1$-P-P)] (P-P = dadpp, dppene)

Solid $Me_3NO \cdot 2H_2O$ (0.0511 g, 0.46 mmol) was added to a continuously stirred solution of [$Re_2(CO)_{10}$] (0.3132 g, 0.48 mmol) in 50 ml of THF at room temperature. The yellow reaction mixture so formed was stirred under reduced pressure. After all the $Me_3NO \cdot 2H_2O$ solid had dissolved, stirring was continued for another 30 min, and half of the solvent was removed under reduced pressure. The remaining solution was stirred for a further 15 min before it was slowly transferred to a stirred solution of the diphosphine (0.44 mmol) in 24 ml of THF via a PTFE transfer tube. The resultant yellow solution was stirred under nitrogen for 1 h. Half of the solvent was then removed and stirring was continued for another 50 min, after which the solution was evaporated to dryness to give a yellow residue.

4.2.1. Workup procedure for P-P = dadpp

The yellow residue was redissolved in a minimum quantity of CH_2Cl_2 and chromatographed on silica TLC plates. Elution with CH_2Cl_2–hexane (1:4) followed by recrystallization from CH_2Cl_2–MeOH yielded 0.050 g (9%) of [$Re_2(CO)_9${P(o-anisyl$)_2(CH_2)_3PPh_2$}] (R_f = 0.48), **1**; 0.039 g (7%) of [$Re_2(CO)_9${$PPh_2(CH_2)_3$-P(o-anisyl$)_2$}] (R_f = 0.25), **2**, and 0.040 g (10%) of [{Re_2-$(CO)_9$}$_2$(μ-dadpp)] **3** (R_f = 0.52).

[$Re_2(CO)_9${P(o-anisyl$)_2(CH_2)_3PPh_2$}], **1** (Found: C, 39.9; H, 2.7. $C_{38}H_{30}O_{11}P_2Re_2$ requires C, 39.6; H, 2.9%); ν_{max}(CO) 2102m, 2032m, 1991s, 1956m, 1931m cm^{-1} (CH_2Cl_2); δ_p ($CDCl_3$) −8.3 (s, Re–P), −17.5 (s, free-P). [$Re_2(CO)_9${$PPh_2(CH_2)_3P(o$-anisyl$)_2$}], **2** (Found: C, 40.2; H, 2.7. $C_{38}H_{30}O_{11}P_2Re_2$ requires C, 39.6; H, 2.9%); ν_{max}(CO) 2104m, 2034m, 1994s, 1958m, 1939m cm^{-1} (CH_2Cl_2); δ_p ($CDCl_3$) −11.7 (s, Re–P), −35.8 (s, free-P). [{$Re_2(CO)_9$}$_2$(μ-dadpp)], **3** (Found: C, 31.5; H, 1.7. $C_{47}H_{30}O_{20}P_2Re_4$ requires C, 31.4; H, 1.8%); ν_{max}(CO) 2104m, 2033m, 1994s, 1958m, 1933m cm^{-1} (CH_2Cl_2); δ_p ($CDCl_3$) 4.3 (s, Ph–P), −5.2 (s, anisyl-P).

4.2.2. Workup procedure for P-P = dppene

About 3 ml of CH_2Cl_2 was added to the yellow residue. A suspension was obtained, which was centrifuged to yield the light yellow [{$Re_2(CO)_9$}$_2$(μ-dppene)] (10%)

solid and a yellow supernatant. The yellow supernatant was chromatographed on silica TLC plates. Elution with CH_2Cl_2–hexane (1:3) followed by recrystallization from CH_2Cl_2–MeOH yielded *eq*-[$Re_2(CO)_9(\eta^1$-dppene)], **4** (15%).

eq-[$Re_2(CO)_9(\eta^1$-dppene)], **4** (Found: C, 40.9; H, 2.1. $C_{35}H_{22}O_9P_2Re_2$ requires C, 41.2; H, 2.2%); ν_{max}(CO) 2103m, 2036m, 1994s, 1959m, 1929m cm^{-1} (CH_2Cl_2); δ_p ($CDCl_3$) −2.6 (d, Re–P), −7.1 (d, free-P), J_{P-P} = 8 Hz. The axial isomer was obtained by boiling a solution of *eq*-**4** in toluene for 10 min under N_2. δ_p ($CDCl_3$) 7.3 (d, Re–P), −6.7 (d, free-P), J_{P-P} = 10 Hz.

[{$Re_2(CO)_9$}$_2$(μ-dppene)] (Found: C, 32.1; H, 1.3. $C_{44}H_{22}O_{18}P_2Re_4$ requires C, 31.8; H, 1.3%); ν_{max}(CO) 2104m, 2038m, 1994s, 1959m, 1938m cm^{-1} (toluene); δ_p (toluene-d_8) 8.6 (s).

4.3. Reactions of [$Re_2(CO)_9(\eta^1$-P-P)] (P-P = dadpp, dppene) with Me_3NO

In a typical experiment, [$Re_2(CO)_9(\eta^1$-P-P)] (0.036 mmol) was dissolved in 5 ml of freshly distilled and degassed THF. A 0.012 M solution of $Me_3NO \cdot 2H_2O$ in THF–MeOH (49:1) mixture (3 ml, 0.036 mmol of Me_3NO) was then added dropwise under nitrogen. The resultant solution was degassed again and stirred under nitrogen for 4 h at room temperature. The solution was then evaporated to dryness and the yellow residue was redissolved in a minimum quantity of CH_2Cl_2 and chromatographed on silica TLC plates.

4.3.1. [$Re_2(CO)_9${P(*o*-anisyl)$_2$(CH_2)$_3$$PPh_2$}] (**1**)

Elution with acetone–hexane (1:3) followed by recrystallization from CH_2Cl_2–hexane yielded [$Re_2(CO)_8$(μdadpp)] (5%, R_f = 0.45) and [$Re_2(CO)_9${P(*o*-anisyl)$_2$(CH_2)$_3$P(O)Ph_2}], **5** (30%, R_f = 0.35).

[$Re_2(CO)_8$(μ-dadpp)] (Found: C, 41.3; H, 2.9. $C_{37}H_{30}O_{10}P_2Re_2$ requires C, 41.6; H, 2.8%); ν_{max}(CO) 2067w, 2031m, 2011w, 1972s, 1947m, 1903s cm^{-1} (CH_2Cl_2); δ_p ($CDCl_3$) −10.4 (d, Ph–P), −20.2 (d, anisyl-P), J_{P-P} = 30 Hz.

[$Re_2(CO)_9${P(*o*-anisyl)$_2$(CH_2)$_3$P(O)Ph_2}], **5** (Found: C, 40.8; H, 2.9. $C_{38}H_{30}O_{12}P_2Re_2$ requires C, 41.0; H, 2.7%); ν_{max}(CO) 2102w, 2031m, 1991s, 1953m, 1931m cm^{-1} (CH_2Cl_2); δ_p ($CDCl_3$) 32.7 (s, P═O), −7.2 (s, Re–P).

4.3.2. [$Re_2(CO)_9${PPh_2(CH_2)$_3$P(*o*-anisyl)$_2$}] (**2**)

Elution with acetone–hexane (1:3) followed by recrystallization from CH_2Cl_2–hexane yielded [$Re_2(CO)_8$(μ-dadpp)] (20%) and [$Re_2(CO)_9${PPh_2(CH_2)$_3$P(O)(*o*-anisyl)$_2$}], **6** (27%, R_f = 0.35) (Found: C, 40.9; H, 2.9. $C_{38}H_{30}O_{12}P_2Re_2$ requires C, 41.0; H, 2.7%); ν_{max}(CO) 2104w, 2033m, 1994s, 1958m, 1936m cm^{-1} (CH_2Cl_2); δ_p ($CDCl_3$) 33.3 (s, P═O), 4.8 (s, Re–P).

4.3.3. eq-[$Re_2(CO)_9(\eta^1$-dppene)], eq-**4**

Elution with ether–hexane (9:1) followed by recrystallization from CH_2Cl_2–hexane yielded 0.0069 g (19%) of [$Re_2(CO)_8$(O═PPh_2CH═CHPPh_2)], **7** (yellow, R_f = 0.71) and 0.0052 g (14%) of *eq*-[$Re_2(CO)_9${PPh_2CH═CHP(O)Ph_2}] (colourless, R_f = 0.55).

[$Re_2(CO)_8$(O═PPh_2CH═CHPPh_2)], **7** (Found: C, 39.8; H, 2.3. $C_{34}H_{22}O_9P_2Re_2$ requires C, 40.4; H, 2.2%); ν_{max}(CO) 2091m, 2052m, 1997s, 1963w, 1935w cm^{-1} (CH_2Cl_2); δ_p ($CDCl_3$) 26.3 (d, O═P), −23.6 (d, Re–P), J_{P-P} = 4.5 Hz; FAB-MS: 1009 (60%, $[M + H]^+$); 981 (10%, $[M + H - CO]^+$); 953 (10%, $[M + H - 2CO]^+$); 925 (40%, $[M + H - 3CO]^+$); 897 (10%, $[M + H - 4CO]^+$); 869 (30%, $[M + H - 5CO]^+$); 841 (10%, $[M + H - 6CO]^+$); 813 (10%, $[M + H - 7CO]^+$); 785 (20%, $[M + H - 8CO]^+$) (masses quoted are those of the [^{185}Re–^{187}Re] ions, which give the strongest peak in each cluster; the relative intensities of the peaks in each cluster are consistent with each cluster being an overlap of the isotope patterns of the $[M + H - nCO]^+$ and $[M - nCO]^+$ ions).

eq-[$Re_2(CO)_9${PPh_2CH═CHP(O)Ph_2}] (Found: C, 40.3; H, 2.0. $C_{35}H_{22}O_{10}P_2Re_2$ requires C, 40.5; H, 2.1%); ν_{max}(CO) 2104w, 2037m, 1995s, 1962m, 1931m cm^{-1} (CH_2Cl_2); δ_p ($CDCl_3$) 22.6 (d, O═P), −5.9 (d, Re–P), J_{P-P} = 36 Hz.

4.3.4. ax-[$Re_2(CO)_9(\eta^1$-dppene)], ax-**4**

Two main product bands were eluted by ether–hexane (9:1). A colourless solid was recovered from the band at R_f = 0.32 by recrystallization from CH_2Cl_2–hexane, and was identified to be *ax*-[$Re_2(CO)_9$-{PPh_2CH═CHP(O)Ph_2}] (0.0030 g, yield 8%). (Found: C, 40.2; H, 2.1. $C_{35}H_{22}O_{10}P_2Re_2$ requires C, 40.5; H, 2.1%); ν_{max}(CO) 2106w, 2036m, 1997s, 1963m, 1939m cm^{-1} (CH_2Cl_2); δ_p ($CDCl_3$) 23.2 (d, O═P), 8.7 (d, Re–P), J_{P-P} = 45 Hz.

An unidentified, unstable yellow compound was recovered from the band at R_f = 0.55. ν_{max}(CO) 2085m, 2044m, 1990s (sh), 1933w cm^{-1} (CH_2Cl_2).

Unreacted *ax*-[$Re_2(CO)_9(\eta^1$-dppene)] was observed on the TLC plates.

4.4. Attempted reaction of free 1,4-bis(diphenylphosphino)butane with Me_3NO

The diphosphine (0.0307 g, 0.072 mmol) was dissolved in 10 ml of freshly distilled and degassed THF. A 0.012 M solution of $Me_3NO \cdot 2H_2O$ in THF–MeOH (49:1) mixture (6 ml, 0.072 mmol of Me_3NO) was then added under nitrogen. The resultant solution was degassed again and stirred under nitrogen at room temperature for 4 h. Analysis of the solution by TLC (ether–hexane, 9:1) showed that no reaction had occurred.

4.5. Preparation of $[NBu_4][ReO_4]$

The compound Re_2O_7 (0.60 g, 1.2 mmol) was dissolved in 3 ml of 1 M aqueous NaOH solution (3 mmol of NaOH). A solution of $[NBu_4]Br$ (1.9 g, 5.9 mmol) in a minimum volume of water was then added dropwise with stirring. The white precipitate obtained was filtered, washed with deionized water, and dried under vacuum to yield 0.8 g (70%) of $[NBu_4][ReO_4]$.

4.6. Reaction of eq-$[Re_2(CO)_9(\eta^1$-dppm)] with $[NBu_4][ReO_4]$

The complex *eq*-$[Re_2(CO)_9(\eta^1$-dppm)] (0.0363 g, 0.036 mmol), prepared as described in [1], was dissolved in 5 ml of freshly distilled and degassed THF. Solid $[NBu_4][ReO_4]$ (0.0177 g, 0.036 mmol) was added under nitrogen. The resultant solution was degassed and stirred under nitrogen for 4 h at room temperature. The solution was then evaporated to dryness and the residue redissolved in a minimum quantity of CH_2Cl_2 and chromatographed on silica TLC plates. Elution with ether–hexane (9:1) followed by recrystallization from CH_2Cl_2–hexane yielded 0.0039 g (15% yield based on the consumed starting material) of *eq*-$[Re_2(CO)_9$(dppmO)] (identified by its ^{31}P NMR spectrum [1]). Unreacted $[Re_2(CO)_9(\eta^1$-dppm)] was also isolated (ca. 0.01 g, 0.01 mmol).

Table 1
Crystallographic data for *eq*-$[Re_2(CO)_9(\eta^1$-dppene)] (**4**)

Empirical formula	$C_{35}H_{22}O_9P_2Re_2$
Formula weight	1020.87
Temperature (K)	293(2)
Wavelength (Å)	0.71073
Crystal system	Monoclinic
Space group	*C*2/*c*
Unit cell dimensions	
a (Å)	35.7794(3)
b (Å)	9.6654(2)
c (Å)	21.0640(3)
β (°)	97.674(1)
Volume (Å^3)	7219.2(2)
Z	8
D_{calc} (Mg/m^3)	1.879
Absorption coefficient (mm^{-1})	6.841
F(000)	3872
Crystal size (mm^3)	0.38 × 0.35 × 0.30
θ Range for data collection (°)	2.18–29.17
Index ranges	$-48 \leqslant h \leqslant 46$, $-13 \leqslant k \leqslant 11$, $-28 \leqslant l \leqslant 26$
Reflections collected	22,822
Independent reflections (R_{int})	8842 (0.0269)
Completeness to theta = 29.17°	90.5%
Maximum and minimum transmission	0.234 and 0.148
Refinement method	Full-matrix least-squares on F^2
Data/restraints/parameters	8842/0/433
Goodness-of-fit on F^2	1.112
Final *R* indices [$I > 2\sigma(I)$]	$R_1 = 0.0288$, $wR_2 = 0.0571$
R indices (all data)	$R_1 = 0.0440$, $wR_2 = 0.0624$
Largest differential peak and hole (e Å^{-3})	0.854 and −1.071

Table 2
Selected bond lengths (Å) and angles (°) for *eq*-$[Re_2(CO)_9(\eta^1$-dppene)] (**4**)

Re(1)–Re(2)	3.1077(2)	Re(2)–C(22)	1.998(5)
Re(1)–P(1)	2.4887(9)	Re(2)–C(23)	2.010(5)
Re(1)–C(11)	1.943(5)	Re(2)–C(24)	2.006(5)
Re(1)–C(12)	1.980(5)	Re(2)–C(25)	1.996(5)
Re(1)–C(13)	1.957(4)	P(1)–C(1)	1.812(4)
Re(1)–C(14)	1.993(5)	P(2)–C(2)	1.826(4)
Re(2)–C(21)	1.945(5)	C(1)–C(2)	1.334(5)
C(11)–Re(1)–P(1)	88.9(1)	C(21)–Re(2)–C(24)	93.7(2)
C(12)–Re(1)–P(1)	86.8(1)	C(22)–Re(2)–C(24)	175.3(2)
C(13)–Re(1)–P(1)	177.8(1)	C(23)–Re(2)–C(24)	85.5(2)
C(14)–Re(1)–P(1)	91.0(1)	C(25)–Re(2)–C(24)	91.4(2)
P(1)–Re(1)–Re(2)	99.79(2)	C(22)–Re(2)–Re(1)	83.3(1)
C(12)–Re(1)–Re(2)	83.1(1)	C(23)–Re(2)–Re(1)	86.5(1)
C(13)–Re(1)–Re(2)	81.2(1)	C(24)–Re(2)–Re(1)	93.0(2)
C(14)–Re(1)–Re(2)	84.2(1)	C(25)–Re(2)–Re(1)	83.6(1)
C(2)–C(1)–P(1)	125.2(3)	C(1)–P(1)–Re(1)	118.6(1)
C(1)–C(2)–P(2)	126.0(3)		

4.7. X-ray crystallography

Single crystals of **4** were grown from CH_2Cl_2–MeOH at ca. 5 °C. The crystal was mounted on a quartz fibre for data-collection on a Bruker SMART CCD system, using Mo Kα radiation, with 6s exposures. Data were corrected for Lorentz and polarization effects with the SMART suite of programs [16], and for absorption effects with SADABS [17]. Structural solution and refinement were carried out with the SHELXTL suite of programs [18]. Final unit cell parameters were determined from 6934 reflections. The structure was solved by direct methods. Hydrogen atoms were placed in idealized positions and refined as riding on their carrier atoms, with the constraint $U_{iso}(H) = 1.2U_{eq}$(carrier). All non-hydrogen atoms were given anisotropic thermal parameters in the final model. Crystallographic data are given in Table 1 and selected bond lengths and angles in Table 2.

5. Supplementary material

Crystallographic data (excluding structure factors) for the structure reported in this paper have been deposited with the Cambridge Crystallographic Data Centre as Supplementary Publication No. CCDC 268940. Copies of the data can be obtained free of charge on application to CCDC, 12 Union Road, Cambridge CB2 1EZ, UK (fax: +44 1223 336 033; e-mail: deposit@ccdc.cam.ac.uk or http://www.ccdc.cam.ac.uk).

Acknowledgements

We acknowledge the financial support (Grant No. RP 15/95 YYK) of the National Institute of Education, Nanyang Technological University (NTU). Wei Fan and Rui Zhang are grateful to NTU for scholarship awards.

References

[1] W. Fan, R. Zhang, W.K. Leong, Y.K. Yan, Inorg. Chim. Acta 357 (2004) 2441.
[2] T.S.A. Hor, H.S.O. Chan, K.-L. Tan, L.-T. Phang, Y.K. Yan, L.-K. Liu, Y.-S. Wen, Polyhedron 10 (1991) 2437.
[3] J.W. Benson, R.L. Keiter, E.A. Keiter, A.L. Rheingold, G.P.A. Yap, V.V. Mainz, Organometallics 17 (1998) 4275, The value of 3.5 Å given in this reference is the distance between the terminal phosphorus and the CO carbon to which the phosphorus lone pair is directed. Data for this structure (Refcode HAQNAO) from the Cambridge Crystallographic Database (Version 5.26, November 2004) showed that another short P(terminal)···C(*cis*-CO) contact of 3.42 Å exists. Two other structures with short P···C contacts were also found in the CCD: $[W(CO)_4(CNCH_2Ph)(\eta^1\text{-dppm})]$ (3.35 Å, Refcode UNAPII) [19] and $[Fe(CO)_4(\eta^1\text{-dppm})]$ (3.43 Å, Refcode JOFJOD) [20].
[4] R.L. Keiter, E.A. Keiter, D.M. Olson, J.R. Bush, W. Lin, J.W. Benson, Organometallics 13 (1994) 3752.
[5] R.L. Keiter, J.W. Benson, Z. Jia, E.A. Keiter, D.E. Brandt, Organometallics 19 (2000) 4518.
[6] R. Zhang, C.L. Kee, W.K. Leong, Y.K. Yan, J. Organomet. Chem. 689 (2004) 2837.
[7] S.D. Christie, M.D. Clerk, M.J. Zaworotko, J. Crystallogr. Spectrosc. Res. 23 (1993) 591.
[8] W.L. Ingham, A.E. Leins, N.J. Coville, S. Afr. J. Chem. 44 (1991) 6.
[9] G.W. Harris, J.C.A. Boeyens, N.J. Coville, J. Chem. Soc., Dalton Trans. (1985) 2277.
[10] T.S.A. Hor, P.M.N. Low, Y.K. Yan, L.-K. Liu, Y.-S. Wen, J. Organomet. Chem. 448 (1993) 131.
[11] G.W. Harris, J.C.A. Boeyens, N.J. Coville, Organometallics 4 (1985) 914.
[12] M.O. Albers, J.C.A. Boeyens, N.J. Coville, G.W. Harris, J. Organomet. Chem. 260 (1984) 99.
[13] M.R. Churchill, K.N. Amoh, H.J. Wasserman, Inorg. Chem. 20 (1981) 1609.
[14] A.J. Gordon, R.A. Ford, The Chemist's Companion: a Handbook of Practical Data, Techniques and References, Wiley-Interscience, New York, 1972.
[15] F.R. Benn, J.C. Briggs, C.A. McAuliffe, J. Chem. Soc., Dalton Trans. (1984) 293.
[16] SMART Software Reference Manual, Version 4.0, Siemens Energy & Automation, Inc., Analytical Instrumentation, Madison, WI, 1996.
[17] G.M. Sheldrick, SADABS, a Software for Empirical Absorption Correction, University of Göttingen, Göttingen, 1996.
[18] SHELXTL Reference Manual, Version 5.03, Siemens Energy & Automation, Inc., Analytical Instrumentation, Madison, WI, 1996.
[19] M. Knorr, I. Jourdain, D. Lentz, S. Willemsen, C. Strohmann, J. Organomet. Chem. 684 (2003) 216.
[20] A.M.G. Dias Rodrigues, J.R. Lechat, R.H.P. Francisco, Acta Crystallogr. C 48 (1992) 159.